Catalysis Today 147S (2009) S176–S184

Contents lists available at ScienceDirect

Catalysis Today

journal homepage: www.elsevier.com/locate/cattod

# Microstructured reactors for diesel steam reforming, water-gas shift and preferential oxidation in the kiloWatt power range

Gunther Kolb *, Christian Hofmann, Martin O'Connell, Jochen Schürer

*Institut für Mikrotechnik Mainz (IMM), Carl-Zeiss-Str.18-20, D-55129 Mainz, Germany*

ARTICLE INFO

*Keywords:*
Steam reforming
Water-gas shift
Preferential oxidation
Microstructured reactors

ABSTRACT

The paper reports from development and testing of three microstructured reactors of the kW scale, namely an oxidative diesel steam reformer, a water-gas shift reactor and a preferential oxidation reactor as first prototypes of a future fuel processor system. The reformer (cubic shape, edge length 80 mm) had a co-current flow arrangement. While oxidative diesel steam reforming was performed in one flow path, the energy supply for this endothermic reaction originated from the combustion of hydrogen in an integrated afterburner. The reactor was operated in the temperature range between 850 °C and 900 °C at S/C ratios between 3.2 and 4.6 and O/C ratios of 0.15–0.2. Full conversion of the diesel fuel could be achieved under all test conditions, however, formation of light hydrocarbons started after some hours of operation at lower S/C ratios.

At this stage of the development, the clean-up reactors were tested separately applying reformate surrogate as feed. The water-gas shift reactor was operated as a counter-current heat-exchanger, which utilized the cathode off-gas of the fuel cell as coolant. This further converted the CO towards the reactor outlet exceeding the equilibrium conversion achievable at the inlet. The reactor was operated at temperatures of up to 400 °C at the inlet and 250 °C at the outlet. Over 90% conversion could be achieved in this single stage water-gas shift reactor.

The second clean-up stage, namely the preferential oxidation reactor, was designed as a co-current heat-exchanger. Water evaporation was chosen as the cooling source. The CO could be reduced under most operating conditions to levels below 100 ppm, which is sufficient to operate a CO-tolerant low temperature PEM fuel cell with the purified reformate.



## 1. Introduction

Idling of trucks for the generation of power when the truck is not in motion has been a common practice especially in the US, where the driver cabins are large and require excessive amounts of electrical power. Because the main engine of the truck is very inefficient when idling and generates about twice as much $NO_x$ compared with driving at 90 km $h^{-1}$ [1,2] this gives rise to a pollution problem. The average idling time amounts to more than 1800 h per vehicle per annum and 3.8 billion L of diesel had been consumed in this manner every year in the US. Consequently, legislation prevents truck idling in most states of the US since the beginning of 2008. Therefore alternative power generation systems or auxiliary power units (APUs) are required. Fuel cell technology promises advantages concerning efficiency, emissions and noise for this application. In case the fuel cell is linked to a diesel fuel processor, the existing fuel infrastructure could be utilized avoiding the distribution issues of alternatives such as compressed hydrogen. Such an application is regarded as niche market with significant potential [3]. Other applications of diesel fuel processor/fuel cell systems are naval systems and, in the case of kerosene, aircrafts [4].

To-date, relatively few diesel reformer reactors and fuel processors have been reported in the open literature. While some applications are based upon partial oxidation of the diesel fuel [5–7], most of them rely on autothermal reforming (ATR) [8–13]. While ATR has the potential for low system complexity and could utilize ceramic or metallic monolithic reactors readily available from automotive exhaust clean-up technology, it suffers from lower efficiency when compared to steam reforming [4,14]. However, the thermal mass of the system, the number of start-up procedures per day, the duration of the system operation and many other factors affect the overall system efficiency as well.

To-date only few diesel fuel processors are known from the open literature, which have worked with steam reforming. Krummrich et al. reported about a diesel 25 kW fuel processor for future application in naval systems [15]. An adiabatic pre-reformer was switched upstream the steam reformer in this

* Corresponding author.
*E-mail address:* kolb@imm-mainz.de (G. Kolb).

0920-5861/$ – see front matter © 2009 Elsevier B.V. All rights reserved.
doi:10.1016/j.cattod.2009.07.003

particular case. Irving et al. presented a multi-fuel processor based upon microstructured reactor technology [16], which was also capable of converting diesel fuel. However, not many details of the reactor design had been disclosed.

The current paper presents results from a microstructured plate-heat-exchanger operating under conditions of oxidative steam reforming, which are still far away from autothermal operation, while the heat was supplied to the reactor by integrated hydrogen combustion as is described in Section 3.

In case PEM fuel cell technology is coupled to the fuel processor, the reformate requires purification from the carbon monoxide formed during the reforming process owing to the limited CO tolerance of the PEM fuel cell anode catalyst. This is usually done by means of catalytic processes, namely water-gas shift (WGS) and preferential oxidation (PrOx) reactions (see also Section 2).

The literature regarding the performance of water-gas shift reactors in the kW scale is rather limited to-date and mostly deals with adiabatic monoliths [17–19] and membrane reactors [20–22].

Apart from an earlier publication of the authors group [23] results from water-gas shift in microchannels were mostly generated in isothermal testing reactors to-date concentrating on catalyst development rather than on a system [24,25].

Similar to water-gas shift, the preferential oxidation reaction requires at least two stages or multiple points of oxygen addition to achieve stable and sufficiently high conversion of the remaining carbon monoxide to levels below 100 ppm as required by the low temperature PEM fuel cell. This applies both for fixed bed reactors [26,27] and monolithic reactors [17,28–31] and increases system complexity and cost.

Plate-heat-exchanger technology has the potential for efficient removal of the heat of the PrOx reaction, which then allows for the utilization of a single stage approach [32,33].

## 2. Reaction system

Diesel fuel is more difficult to reform compared to alcohols and lighter hydrocarbon mixtures owing to coke formation issues, which may occur during its injection into the feed mixture or over the catalyst downstream. To prevent the latter, reaction temperatures exceeding 800 °C should be envisaged, which needs to be taken into consideration when choosing the catalyst formulations. The catalyst itself needs to be resistant to sintering at these elevated temperatures.

To generate hydrogen from fossil hydrogen carriers, steam and/or air can be added to the reformer feed, which corresponds then to steam reforming, partial oxidation and autothermal reforming processes. Only in the case that the reformer works in a thermally neutral manner should oxidative steam reforming be named autothermal reforming and corresponds to an atomic O/C ratio between 0.7 and 0.9 depending on the diesel feedstock and the experimental factors such as quality of insulation, which determines the heat losses of the system of course. In the event of lower oxygen addition than is required for autothermal conditions, the oxidative steam reforming is still endothermic and requires external energy input. Such conditions were chosen for the reactor here and the additional energy was generated by an integrated afterburner as described in Section 3.

The diesel fuel applied for the experiments presented in the current paper was pseudo Euro V diesel supplied from Shell, which could be described by the simplified overall formula $C_{11.3}H_{24.6}$. However, analyses confirmed the presence of a significant amount of aromatics in this feedstock and therefore the hydrogen number is in fact lower.

Calculations from Aspen® modelling software revealed the following scheme for oxidative diesel steam reforming, performed at S/C 3, O/C 0.3 and 800 °C:

$$C_{11.3}H_{24.6} + 1.7O_2 + 33.9H_2O \rightarrow 6.0CO + 5.3CO_2 + 25.5H_2 + 20.7H_2O \quad \Delta H_{1073\,K} = 853\,\text{kJ/mol} \tag{1}$$

In Eq. (1) the equilibrium of the water-gas shift reaction is taken into consideration, while the methanation reaction is not included. However, owing to the thermodynamic equilibrium, formation of methane is only minor according to thermodynamics at temperatures exceeding 800 °C [4]. Nevertheless methane might be formed depending on the catalyst formulation.

The carbon monoxide clean-up reactions will be discussed only briefly below. Water-gas shift is usually performed in two stages at temperatures around 375–450 °C in the first stage and between 200 °C and 300 °C in the second [4]:

$$CO + H_2O \leftrightarrow CO_2 + H_2 \quad \Delta H_{298\,K} = -41\,\text{kJ/mol} \tag{2}$$

The reactor presented here was rather a medium temperature shift reactor coated with suitable catalyst and operated between 420 °C at the temperature maximum and 250 °C at the outlet.

The preferential oxidation of carbon monoxide is highly exothermic and accompanied with unselective and parasitic hydrogen oxidation:

$$CO + 0.5O_2 \rightarrow CO_2 \quad \Delta H_{298\,K} = -283\,\text{kJ/mol} \tag{3}$$

$$H_2 + 0.5O_2 \rightarrow H_2O \quad \Delta H_{298\,K} = -242\,\text{kJ/mol} \tag{4}$$

Usually an excess of oxygen is required to achieve the desired high degree of conversion.

## 3. Fuel processor concept and design of the reactors

### 3.1. Flow scheme of the planned fuel processor

The concept of the auxiliary power unit, for which the reactors discussed here were designed as first stage prototypes is shown in Fig. 1. A low temperature PEM fuel cell with reformate tolerant anode catalyst is supplied with purified reformate from the microstructured fuel processor.

The fuel processor is composed of an oxidative steam reformer (STR) which gains the energy for the steam reforming reaction mainly from combustion of the anode off-gas in an integrated afterburner (AFB). This anode off-gas is pre-heated in a heat-exchanger (HX-1), which cools the reformate downstream the reformer at the same time. Part of the cathode off-gas, pre-heated firstly in heat-exchanger HX-04 and then in the water-gas shift reactor, is utilized as the oxygen source for the combustion reaction in the afterburner. The steam for the reforming reaction is raised mainly in the evaporator, which is supplied with energy from an integrated heat-exchanger utilising the afterburner off-gas heat.

The catalytic carbon monoxide clean-up is performed in a single stage water-gas shift reactor (WGS), designed as a counter-current heat-exchanger and in a preferential oxidation reactor (PrOx) cooled in a co-current flow arrangement by water evaporation. The steam generated in the PrOx reactor is added to the steam reformer feed. On top of diesel and steam feed, a small amount of air is fed to the oxidative steam reformer, which is well beyond the air required to achieve conditions of autothermal reforming.

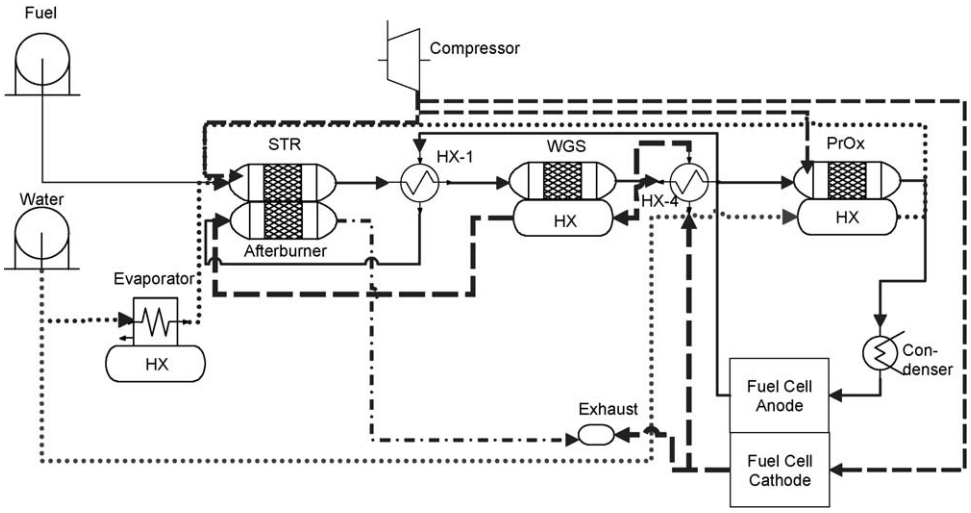


**Fig. 1.** Flow scheme of the fuel processor design; straight lines: fuel; dashed lines: air/cathode off-gas; dotted lines: water/steam; dotted/dashed lines: afterburner off-gas.

**Table 1**
Summary of the dimensions of the reactor: the channel dimensions are only provided for the reformate side of the plates.

| Reactor | STR/AFB | WGS | PrOx |
|---|---|---|---|
| Maximum operating temperature [°C] | 900 | 425 | 200 |
| Maximum operating pressure [bar] | 2 | 2 | 2 |
| Plate size ($L \times W \times H$) [mm] | $80 \times 53 \times 0.8$ | $145 \times 75.8 \times 0.6$ | $175 \times 40 \times 0.6$ |
| Number of half-channels per plate | 45 | 60 | 39 |
| Number of reformate channel levels | 32 | 12 | 32 |
| Channel dimensions ($L \times W \times H$) [mm] | $80 \times 0.8 \times 0.55$ | $125 \times 1 \times 0.65$ | $143 \times 0.8 \times 0.45$ |
| Number of plates | 60 | 36 | 96 |
| Plate stack dimensions including top/bottom plates and temperature measurement [mm] | $80 \times 53 \times 57.6$ | $145 \times 75.8 \times 35.2$ | $193 \times 40 \times 63.6$ |

### 3.2. Reactor design

The reactors were designed as plate-heat-exchangers composed of stainless steel metal foils (German steel code 1.4841). The microstructures were introduced by wet chemical etching into the stainless steel from both sides. The channels were coated with catalyst for diesel steam reforming, anode off-gas combustion, water-gas shift and preferential oxidation respectively by Johnson Matthey Fuel Cells. Subsequently the plates were stapled and sealed by laser welding before the manifolds were attached to the plate stack by laser welding. The size and number of channels and plates are summarized in Table 1.

#### 3.2.1. Design of the diesel steam reformer

The design of the STR/AFB is shown in Fig. 2a. The diesel/steam mixture is fed to the reactor inlet, which has a trumpet shape. This shape was chosen from CFD-simulations to avoid the formation of eddies, which could cause coke build-up by diesel hitting the reactor inlet wall. At the reactor inlet air is added to the feed. The reformate passes straight through the reactor. Anode and cathode off-gas enter the reactor separately and from both sides to gain an even temperature distribution over the reactor width. It had been foreseen to mix both gases inside the reactor. However, as reported in Section 4.1, this was only possible to a certain extent. Similar to the inlet, the afterburner off-gases leave the reactor at both sides.

Six thermocouples could be inserted into the reactor at different positions over the reactor width and length. These positions for temperature measurement were introduced at three levels of the reactor summing up to a total of 18 thermocouples. A photograph of the assembled reactor had been published elsewhere [34]. The plates of the reformer carried steam reforming catalyst on one side,

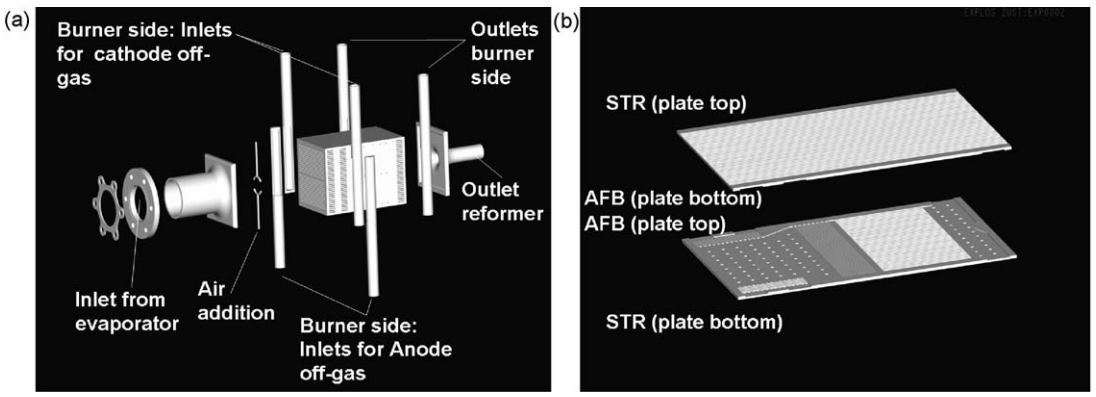


**Fig. 2.** (a) (Left) Explosion view of the STR/AFB and (b) (right) sandwich design of STR and AFB plates.

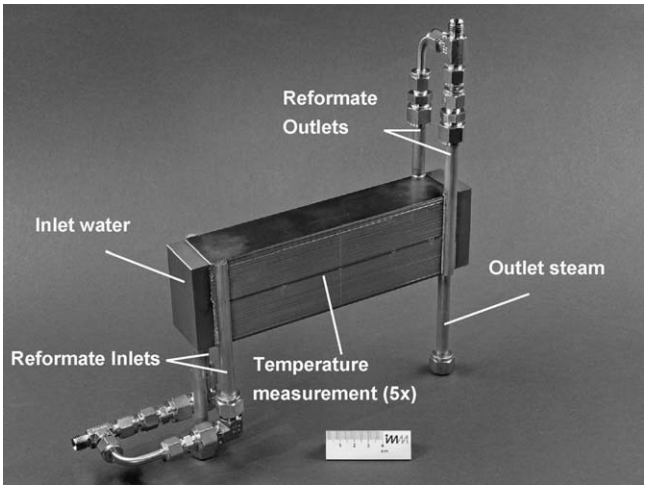


**Fig. 3.** Preferential oxidation reactor.

while combustion catalyst was deposited on the other side thus allowing for a direct coupling of the exothermic and endothermic reactions (see Fig. 2b).

*3.2.2. Design of the water-gas shift reactor*

The design of the water-gas shift reactor is much simpler compared to the diesel reformer. It is a counter-current heat-exchanger having one inlet and outlet for the reformate and for the cathode off-gas each. Five temperatures could be measured over the reactor length axis, both in the reactor core and in the shell. A photograph of the assembled reactor has been published elsewhere [34].

By adjusting a descending temperature profile over the reactor length axis, the equilibrium of the water-gas shift reaction is moved towards lower values of carbon monoxide at the reactor outlet, which favours the degree of conversion achievable [35,36].

*3.2.3. Design of the preferential oxidation reactor*

The highly exothermic carbon monoxide oxidation reaction, which is accompanied by unselective hydrogen oxidation generates significant heat in the preferential oxidation reactor. Owing to the high rate of reaction, this heat is preferably formed at the reactor inlet. To remove the heat, evaporation cooling was chosen in a co-current flow arrangement [37].

As shown in Fig. 3, the reformate enters the preferential oxidation reactor from both sides, while the water is distributed in a front pocket at the reactor inlet. Similar to the inlet, the purified reformate leaves the reactor at both sides, while the superheated steam is gathered in a single outlet manifold. Six thermocouples could be inserted at different positions over the reactor length axis.

## 4. Reactor testing

### 4.1. Experimental

In the case of steam reformer testing, the steam feed was superheated to temperatures of up to 800 °C in an electrically heated gas-heater. This steam was then fed to the diesel injection system (developed by ADROP Feuchtemesstechnik GmbH). The AFB side of the reactor was fed by surrogates of cathode off-gas (oxygen deficient air) and anode off-gas (mainly hydrogen, nitrogen and carbon dioxide), which were pre-heated separately.

Surrogates of reformate equivalent to reformer and water-gas shift reactor off-gas for WGS and PrOx reactor testing respectively were prepared by dosing $H_2$, CO, $CO_2$ (and $N_2$ and $O_2$ in case of PrOx) separately applying thermal mass flow meters and then mixed and pre-heated in electrically supplied gas-heaters. Then steam was blended with the gas and the mixture was further heated to the final feed temperature of the reformate. For cooling, $N_2$ (as surrogate for cathode off-gas, but with the same heat capacity flow in the case of WGS) or deionised water (in the case of PrOx) was fed to the reactors.

On-line GC-analysis was provided by a micro-GC, which allowed for fast analysis cycles of 70 s, enabling rapid monitoring of the reactor performance. The gas composition could only be analysed water-free, thus analysis results are presented on a dry basis (d.b.). Details of the analytical equipment are provided elsewhere [38].

### 4.2. Diesel oxidative steam reformer

The STR/AFB reactor had no electrical heating and therefore it was pre-heated first with nitrogen to a temperature of about 400 °C and then with hot steam up to 600 °C. At this temperature hydrogen combustion was started and the final operating temperature could be reached.

The steam reformer reactor was operated for 45 h under conditions of steam reforming, among them for 35 h under stable conditions at diesel flow rates between 183 g/h and 200 g/h, the second value corresponds to a thermal energy of the hydrogen and carbon monoxide (the latter would be converted to hydrogen in a future fuel processor) produced of 2300 W or an net electrical output of 920 W of the corresponding fuel cell assuming 80% hydrogen utilization and 50% fuel cell efficiency. The energy required for the steam reforming reaction amounted to 400 W, which was transferred from the afterburner side of the reactor. The S/C ratio was varied between 4.6 and 3.2, while the O/C ratio was never increased above 0.2 as summarized in Table 2. The composition of the reformate, which is also provided in Table 2, showed the expected changes corresponding to the experimental conditions. When decreasing the S/C ratio, the hydrogen content of the dry reformate decreased slightly, while the content of carbon monoxide increased by the same amount as the carbon dioxide

**Table 2**
Experimental conditions and gas compositions as determined in the STR/AFB reactor.

| *m* (diesel) [g/h] | S/C | O/C | *p* [bar] | $H_2$ [vol.%], d.b. | $CO_2$ [vol.%], d.b. | CO [vol.%], d.b. | $CH_4$ [vol.%], d.b. | $N_2$ [vol.%], d.b. |
|---|---|---|---|---|---|---|---|---|
| 183 | 4.6 | 0 | 1.3 | 72 | 15.6 | 12.9 | 0.005 | 0 |
| 183 | 4.1 | 0 | 1.3 | 71.8 | 15.2 | 13.4 | 0.02 | 0 |
| 200 | 4.1 | 0 | 2.0 | 71.8 | 15.2 | 13.4 | 0.06 | 0 |
| 200 | 3.9 | 0 | 2.0 | 71.7 | 14.6 | 13.9 | 0.2 | 0 |
| 200 | 3.6 | 0 | 2.0 | 71.5 | 14.2 | 14.5 | 0.15 | 0 |
| 200 | 3.6 | 0.12 | 2.0 | 65.1 | 13.1 | 14.1 | 0.2 | 6.8 |
| 200 | 3.2 | 0.165 | 2.0 | 63.1 | 12.1 | 15.2 | 0.15 | 8.9 |
| 200 | 3.2 | 0.2 | 2.0 | 61.5 | 12.1 | 14.9 | 0.15 | 10.6 |

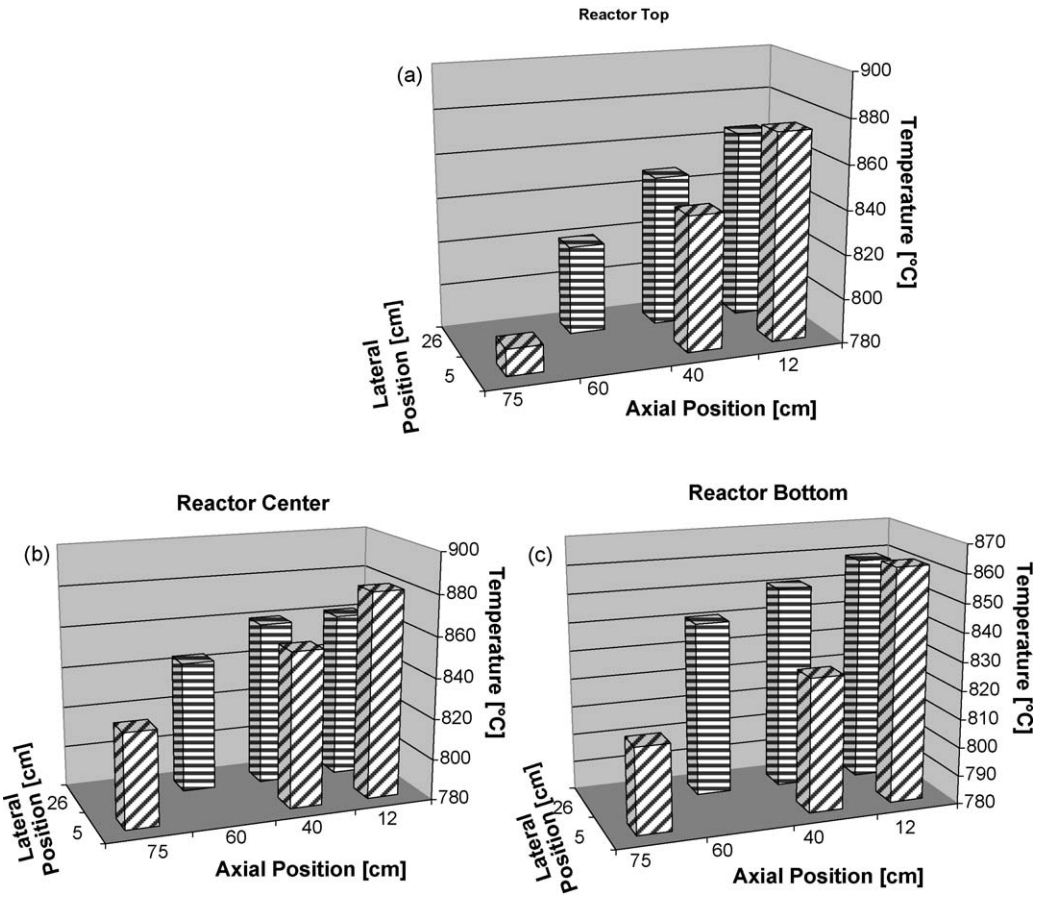


**Fig. 4.** (a–c) Temperature profile of the STR/AFB in axial and lateral direction; top (a): reactor top; bottom left (b): reactor centre; bottom right (c): reactor bottom.

content decreased. When increasing the system pressure from 1.3 bar to 2.0 bar, the content of methane increased owing to the equilibrium of the methanation reaction. At lower values of S/C of 3.6 and 3.2, air was added, which lowered the concentration of all product gases owing to the dilution with nitrogen.

Unconverted diesel could not be detected by the on-line GC but the very small amounts of unconverted hydrocarbons, which could be gathered on top of the product water of each run were measured volumetrically and the conversion of diesel fuel was calculated by these means. It revealed in all cases, that the conversion exceeded 99.9%. GC–MS analysis of the unconverted liquid feedstock indicated a shift towards higher hydrocarbons compared to the composition of the EURO V diesel.

The reactor temperature profile as determined by the 18 thermocouples inserted into the reactor is shown in Fig. 4a–c. It revealed decreasing temperatures from the inlet of the heating gas (front right in Fig. 4a–c), towards the reactor centre (back right in Fig. 4a–c), where most of the heat of the steam reforming reaction was consumed. Generally the temperature decreased towards the reactor outlet (left in Fig. 4a–c). However, the maximum temperature difference from the average value amounted to ±45 K, which is regarded as low considering the high values of temperature.

The GC-analysis of the reformate revealed only carbon oxides, hydrogen and minor amounts of methane as long as the reactor was operated at S/C ratios higher than 4. However, below that value formation of light hydrocarbons, namely ethylene and propylene was observed after a few hours of operation as shown in Fig. 5 for a S/C ratio of 3.6. In parallel, the content of methane in the reformate increased continuously from the very beginning of the test run.

Similar linear increase of light hydrocarbons has been observed by other authors [39,40] and is attributed to catalyst deactivation.

Because the amount of light hydrocarbons initially returned to low values when a new experimental test was started, the deactivation was attributed to coke formation. The coke was obviously partially removed when the reactor was treated with steam during the pre-heating phase of each experiment. It was assumed, that the addition of oxygen to the feed could suppress the deactivation procedure [40]. As shown in Fig. 6, this was the case at an even lower S/C ratio of 3.2. Increasing the O/C ratio from 0.165 to 0.2 further reduced the speed of the deactivation procedure.

It should be mentioned, that the diesel injection system operated in a stable manner during the course of the experiments. It is assumed by the authors, that the diesel/steam mixture was much less subject to coke formation issues compared to conditions of autothermal reforming or even partial oxidation, which require sophisticated design of the injection system [7,39,41] or even application of alternative techniques such as cool flames [42] owing to the coke formation potential of diesel in the presence of oxygen under the conditions applied.

While the diesel steam reforming side of the reactor showed good performance as summarized above, the afterburner side of the reactor suffered from problems concerning the mixing of hydrogen and oxygen in the internal mixing structures of the device. Problems with incomplete combustion of hydrogen at temperatures of 800 °C had not been expected but created problems owing to hydrogen combustion and hot spot formation in the tubing downstream the reactor. To overcome this problem hydrogen was added to the cathode feed of the afterburner, the hydrogen content of the anode feed was reduced and oxygen was added to the anode feed in such a manner, that the adiabatic

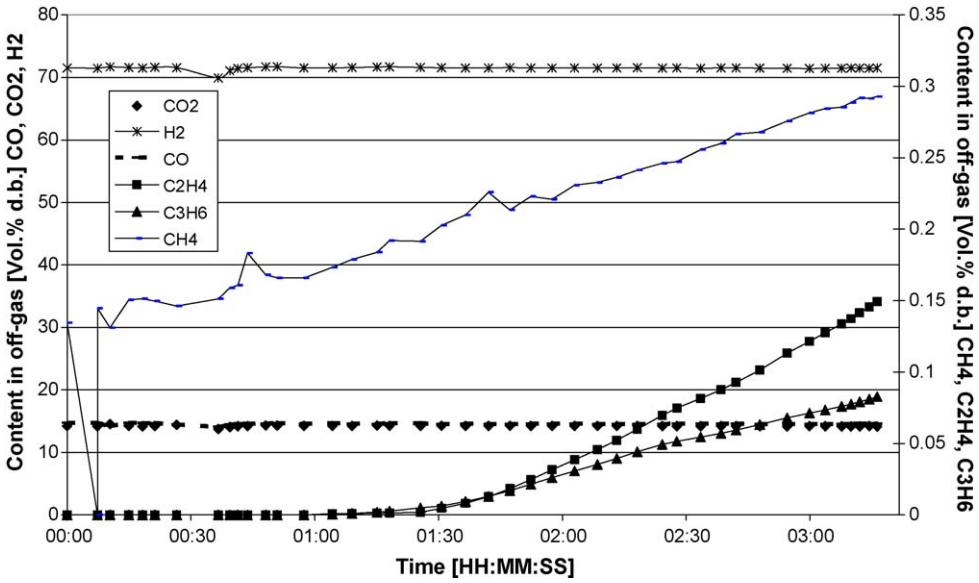


**Fig. 5.** Reformate composition during stable operation at diesel mass flow rate: 200 g/h; S/C = 3.6; O/C = 0.0.

temperature rise of both feed mixtures never exceeded 1000 °C. Consequently homogeneous reactions occurred in the anode and cathode feed tubing right upstream the reactors. This homogeneous combustion was, however, never as hazardous as an oxyhydrogen mixture would be, because the gases were diluted by carbon dioxide and steam in the case of the anode feed and by nitrogen and steam in the case of the cathode feed.

### 4.3. Water-gas shift reactor

The testing conditions and experimental results as generated at the water-gas shift reactor are summarized in Table 3. The reactor was tested at two different flow rates of the reformate surrogate feed, namely 42.4 L/min and 60.1 L/min, which contained 10.1 vol.% and 10.6 vol.% CO respectively on a wet basis. These CO concentrations are very close to the values found for the STR/AFB off-gas as discussed above. The thermal energy of the hydrogen and carbon monoxide processed at the higher flow rate amounted to 4.1 kW. 94% conversion could be achieved at the lower reformate flow rate and 73 L/min flow rate of the cooling air, which corresponds to a CO content of 0.6 vol.% on a wet basis in the purified reformate (first column in Table 3). At the higher reformate flow rate, the conversion was lower and in the range of 90%, which corresponds to a CO content of 1.1 vol.% in the reactor off-gas. Similar degrees of conversion were achieved at different reformate inlet temperatures, cooling air flow rates and cooling air temperatures (third, fourth and sixth columns in Table 3). Changing the reformate pressure from 1.4 bar to 2.0 bar did not affect the reactor performance as was expected (fifth column in Table 3). The degree of conversion achieved in the current single stage reactor is in the same range as it had been determined by Pasel et al. in their two stage monolithic system [18].

Fig. 7 shows the temperature profile both in the reactor core and shell. Obviously owing to heat losses to the environment the shell temperature was slightly lower than the core temperature. The

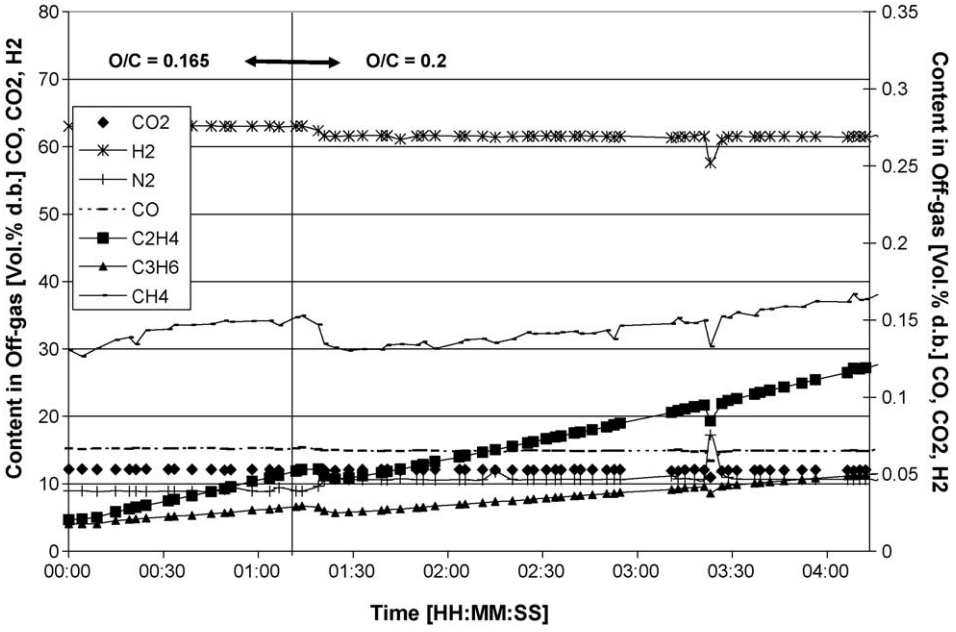


**Fig. 6.** Reformate composition during stable operation at a diesel mass flow rate of 200 g/h; S/C = 3.2; O/C = 0.165/0.2.

**Table 3**
Summary of experimental conditions and results from testing of the water-gas shift reactor.

| Feed composition | | | | | | | |
|---|---|---|---|---|---|---|---|
| $H_2$ | [vol.% w.b.] | 39.2 | 39.2 | 41.3 | 41.3 | 41.3 | 41.3 |
| CO | [vol.% w.b.] | 10.1 | 10.1 | 10.6 | 10.6 | 10.6 | 10.6 |
| $CO_2$ | [vol.% w.b.] | 7.3 | 7.3 | 7.7 | 7.7 | 7.7 | 7.7 |
| $N_2$ | [vol.% w.b.] | 4.2 | 4.2 | 4.5 | 4.5 | 4.5 | 4.5 |
| $H_2O$ | [vol.% w.b.] | 39.2 | 39.2 | 36.0 | 36.0 | 36.0 | 36.0 |
| Total flow rate reformate | [L/min] | 42.4 | 42.4 | 60.1 | 60.1 | 60.1 | 60.1 |
| Pressure reformate | [bar] | 1.4 | 1.4 | 1.4 | 1.4 | 2.0 | 1.4 |
| $T_{Inlet}$ reformate | [°C] | 347 | 358 | 360 | 360 | 360 | 350 |
| $T_{Outlet}$ reformate | [°C] | 260 | 250 | 250 | 240 | 240 | 235 |
| CO content WGS off-gas | [vol.% w.b.] | 0.6 | 0.8 | 1.05 | 1.1 | 1.1 | 1.1 |
| CO conversion | [%] | 94 | 92 | 90 | 89 | 89 | 90 |
| Cooling gas flow rate | [L/min] | 73 | 62 | 87 | 87 | 87 | 67 |
| $T_{Inlet}$ cooling gas | [°C] | 244 | 218 | 220 | 200 | 200 | 160 |
| $T_{Outlet}$ cooling gas | [°C] | 362 | 375 | 375 | 375 | 375 | 375 |

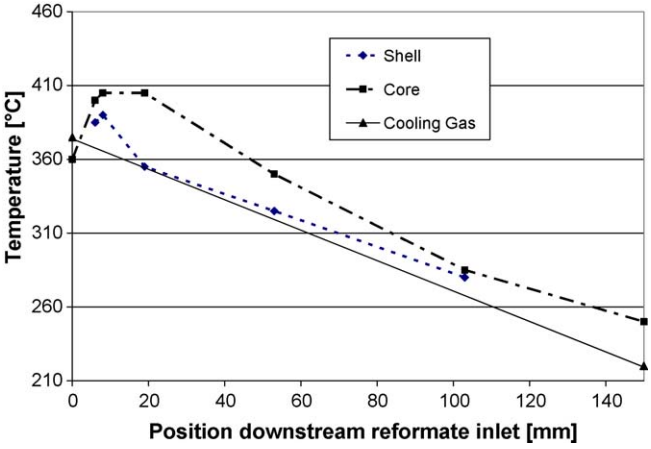


**Fig. 7.** Axial temperature profile over the water-gas shift reactor; total reformate flow: 60.1 L/min; cooling gas flow: 87 L/min; cooling gas inlet temperature: 220 °C.

axial temperature profile of the reactor showed the desired shape. At the inlet, a temperature peak was observed stemming from the heat of the water-gas shift reaction, which generated high initial conversion. Downstream the temperature decreased owing to the heat removal by the cooling air. The total amount of heat which could be removed from the reformate was calculated to 286 W (at the reformate flow rate of 60.1 L/min, cooling gas flow rate of 87 L/min and 220 °C inlet temperature, third column in Table 3). Owing to the initial temperature peak at the reactor inlet, the cooling gas outlet temperature exceeded the reformate inlet temperature, which is not feasible in a normal heat-exchanger, but was in the current heat-exchanger/reactor.

### 4.4. Preferential oxidation reactor

The flow rate of the reformate surrogate fed to the PrOx reactor was changed from 42 N dm$^3$/min to 99 N dm$^3$/min, the CO concentration in the feed was set to either 0.47 vol.% or 0.96 vol.% and the O/CO ratio (λ-value) increased from 2 to 4 so as to assess the performance of the reactor. A feed flow rate which varied from 46 N dm$^3$/min to 57 N dm$^3$/min (the exact number depending on the λ-value) corresponded to 29% of the reformate flow in a final 5 $kW_{el}$ system. Under these conditions the prototype reactor worked as a 1.44 kW PrOx reactor. Feed flow rates around 90–100 N dm$^3$/min corresponded to a 2.5 kW PrOx reactor.

A typical gas feed composition setting was the following 44.40 vol.% $H_2$, 0.47 vol.% CO, 15.25 vol.% $CO_2$, 7.47 vol.% $N_2$, 0.49 vol.% $O_2$ and 31.92 vol.% $H_2O$. Generally speaking, the following four temperature windows were set, 120–140 °C, 140–160 °C, 160–180 °C and 180–200 °C. The reactor temperature window was varied by changing the reformate feed temperature or the flow of cooling water. However, for higher flow rates and higher CO feed concentrations, some temperature windows could not be realised, because the cooling was not sufficient. This was the case especially for higher λ-values, defined here as O/CO, which was as expected since more unselective hydrogen combustion energy is present in the system at higher λ-values. The pressure on the reformate side was 2 bar at all times.

Fig. 8a demonstrates the stable operation and the narrow temperature window of 10 K, which could be adjusted inside the

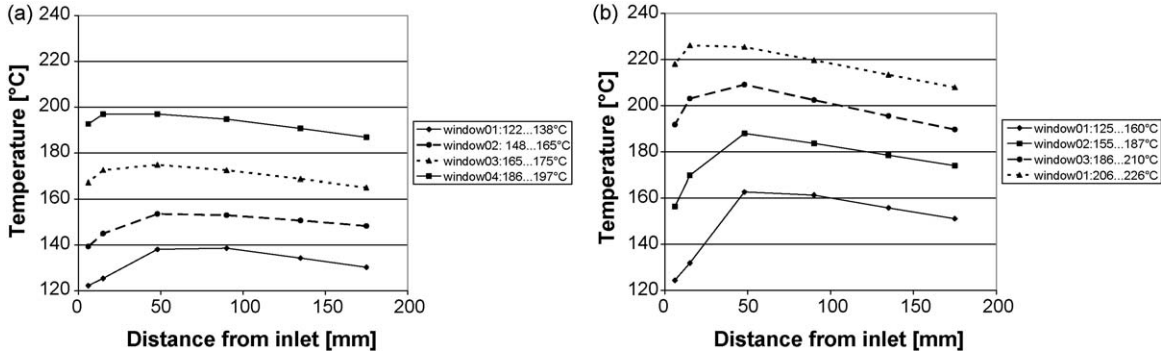


**Fig. 8.** (a and b) Axial temperature profiles over the preferential oxidation reactor; (a) (left) total reformate flow: 46.0 L/min; CO inlet concentration: 0.47 vol.%; O/CO = 2.0; (b) (right) total reformate flow: 54.0 L/min; CO inlet concentration: 0.96 vol.%; O/CO = 2.0.

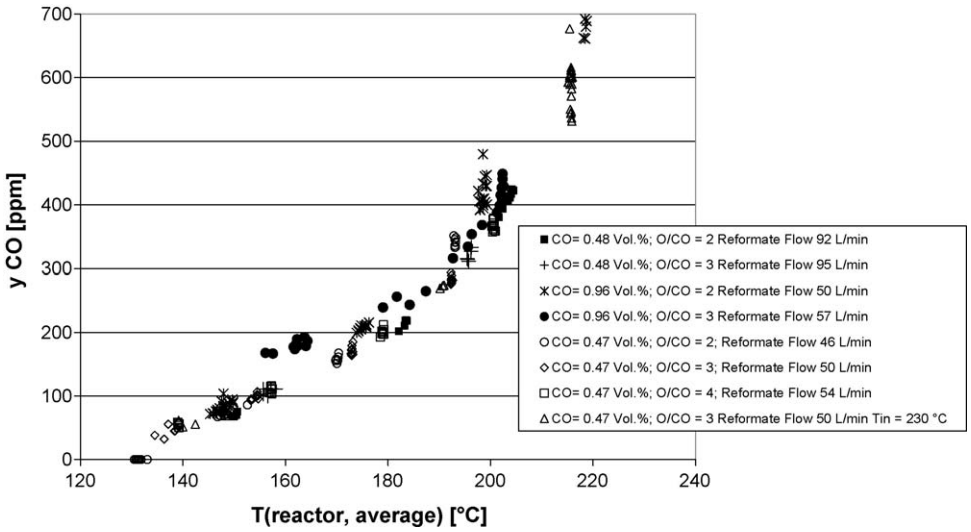


**Fig. 9.** CO concentration in the off-gas of the preferential oxidation reactor at different total reformate flow rates, CO inlet concentrations and O/CO-values.

reactor at least for lower λ-values, i.e. O/CO = 2. 122 g/h water was fed at a pressure of 1.6 bar to the integrated evaporator/cooler under these conditions. The steam left the superheating channels with a temperature of approximately 175 °C, which is about 10 K below the temperature of the reformate outlet. The heat removal by water evaporation and superheating amounted to 94 W under these conditions, which corresponded well with the heat generation of 88 W by hydrogen and carbon monoxide combustion. The remaining cooling power was required to cool the reformate to the off-gas temperature of the reactor. The temperature windows got wider with increasing CO concentration of the reactor feed (see Fig. 8b) and with increasing O/CO-values. At the highest temperature window, the difference in temperature as a function of increasing O/CO was 17 K. It should also be noted that on increasing the temperature window, the hot zone in the reactor shifted towards the inlet. Fig. 9 shows a plot of the CO concentration as determined in the PrOx reactor off-gas over the reactor temperature (average values were chosen) for different experimental conditions. Surprisingly, it is clearly demonstrated, that the off-gas concentration does not decrease with increasing O/CO-values but is only dependant on the reactor temperature.

Thus a higher surplus of air (higher O/CO-value) does not improve the reactor performance. On the contrary, the lowest values (below detection limit, which amounts to 5 ppm for the micro-GC) were found for the O/CO-value of 2, because a lower reactor temperature could be achieved owing to the lower heat generation. Higher temperatures might favour the reverse water-gas shift reaction leading to higher CO content of the purified reformate. However, in this system, complete conversion was achieved at O/CO = 3, in the temperature range between 81 °C and 93 °C. A set of data shown in Fig. 9 was determined for a CO concentration of 0.5 vol.% and flow rates between 46 N $dm^3$/min and 54 N $dm^3$/min. Another set of data is also included which was determined for a reformate feed temperature of 230 °C and a O/CO-value of 3. This corresponded to the assumption, that the reformate is not cooled when leaving the WGS reactor in a finished fuel processing unit. In any case, even at this higher inlet temperature, the reactor was still capable of reducing the CO concentration to below 100 ppm.

In summary, for reformate flow rates of about 50 L/min and an inlet CO concentration of 0.5 vol.%, the reactor could be cooled to an average temperature below 150 °C with the CO concentration decreasing to less than the target of 100 ppm at the reactor outlet for all O/CO-values and reformate feed temperatures. When the CO inlet concentration was increased to 1.1 vol.%, CO levels of 100 ppm and lower were more difficult to attain, as can also be seen in Fig. 9. Only for a O/CO-value of 2, was the reactor capable of reducing the CO concentration to levels below 100 ppm at the reactor outlet.

For a O/CO-value of 3, the amount of CO was greater than 200 ppm. For a O/CO-value of 4, no stable operation of the reactor could be achieved.

When the reformate flow rate was increased to more than 90 L/min, satisfactory results were achieved when the CO inlet concentration was 0.5%. When O/CO was set to 2, levels of 100 ppm were attainable whereas at O/CO = 3, this was slightly above 100 ppm.

When the CO inlet concentration was increased to 1% (not shown in Fig. 9), it proved to be very difficult to control the reactor temperature at these higher settings with the result that CO in the off-gas stream rose to 400 ppm. It is generally believed CO preferential oxidation is also accompanied by the reverse water-gas shift reaction and that the effect is most pronounced when the temperature gradients in a reactor become larger [43].

## 5. Conclusions and outlook

The experiments proved the potential of microstructured plate-heat-exchanger technology for improved heat management and system integration for portable, mobile and distributed stationary fuel processors. As a conclusion of the experiments presented here, the reformer prototype was re-designed and scaled up to a power equivalent of 5 $kW_{el}$ of the corresponding fuel cell, which will be reported elsewhere [44]. The internal mixers of the current reactor were substituted by external mixing chambers, which solved the issue of incomplete hydrogen combustion. Further efforts were made to achieve on-line analysis of the unconverted diesel fuel for these experiments.

The water-gas shift and preferential oxidation reactors presented here were, in parallel to the diesel reformer mentioned above, scaled up to the 5 $kW_{el}$ size and results from their testing will be reported in another subsequent paper [45].

## Acknowledgements

The research presented in this study was performed with funding provided by the European Commission in the scope of the 6th Framework Project, HyTRAN (“Hydrogen and Fuel Cell

Technologies for Road Transport''), contract no. TIP3-CT-2003-502577.

## References


[1] F. Baratto, U.M. Diwekar, D. Manca, J. Power Sources 139 (2005) 214.
[2] H. Lim, Study of Exhaust Emissions from Idling Heavy-duty Diesel Trucks and Commercially Available Idle-reducing Devices, US Environmental Protection Agency, 2002.
[3] P. Agnolucci, W. McDowall, Technol. Forecast. Soc. Change 74 (2007) 1394.
[4] G. Kolb, Fuel Processing for Fuel Cells, Wiley–VCH, Weinheim, 2008.
[5] R. Bosch, Perspective on fuel cells vs. incumbent technologies, in: Fuel Cell Seminar, Palm Springs, California, 2005.
[6] S. Roychoudhury, M. Lyubovski, D. Walsh, D. Chu, E. Kallio, J. Power Sources 160 (2006) 510.
[7] A. Lindermeir, S. Kah, S. Kavurucu, M. Mühlner, App. Catal. B: Environ. 70 (2007) 488.
[8] B. Lenz, T. Aicher, J. Power Sources 149 (2005) 44.
[9] F. Rosa, E. Lopez, Y. Briceno, D. Sopena, R.M. Navarro, M.C. Alvarez-Galvan, J.L.G. Fierro, C. Bordons, Catal. Today 116 (2006) 324.
[10] R. Sopena, A. Melgar, Y. Briceno, R.M. Navarro, M.C. Alvarez-Galvan, F. Rosa, Int. J. Hydrogen Energy 32 (2007) 1429.
[11] J. Pasel, J. Meissner, Z. Pors, R.C. Samsun, A. Tschauder, R. Peters, Int. J. Hydrogen Energy 32 (2007) 4847.
[12] M. Nilsson, X. Karatzas, B. Lindström, L.J. Petterson, Chem. Eng. J. 142 (2008) 309.
[13] D. Chrenko, J. Coulie, S. Lecoq, M.C. Pera, D. Hissel, Int. J. Hydrogen Energy 34 (2009) 1324.
[14] A. Cutillo, S.A. Specchia, M.G. Saracco, V. Specchia, J. Power Sources 154 (2006) 379.
[15] S. Krummrich, B. Tuinstra, G. Kraaij, J. Roes, H. Olgun, J. Power Sources 160 (2006) 500.
[16] P.M. Irving, W. Lloyd Allen, T. Healey, W.J. Thomson (Eds.), Catalytic Micro Reactor Systems for Hydrogen Generation, Springer-Verlag, Berlin, 2001.
[17] C. Severin, S. Pischinger, J. Ogrzewalla, J. Power Sources 145 (2005) 675.
[18] J. Pasel, R.C. Samsun, D. Schmitt, R. Peters, D. Stolten, J. Power Sources 152 (2005) 189.
[19] M. Dokupil, C. Spitta, J. Mathiak, P. Beckhaus, A. Heinzel, J. Power Sources 157 (2006) 906.
[20] G. Barbieri, P. Bernardo, R. Mattia, E. Drioli, R. Bredesen, H. Klette, Chem. Eng. Trans. 4 (2004) 55.
[21] I. Osemwengie, R. Enick, R. Killmeyer, B. Howard, B. Morreale, M. Ciocco, J. Membr. Sci. 298 (2007) 14.
[22] G. Barbieri, A. Brunetti, G. ricoli, E. Drioli, J. Power Sources 182 (2008) 160.
[23] G. Kolb, T. Baier, J. Schürer, D. Tiemann, A. Ziogas, S. Specchia, E. Galetti, G. Germani, Y. Schuurman, Chem. Eng. J. 138 (2008) 474.
[24] G. Germani, P. Alphonse, M. Courty, Y. Schuurman, C. Mirodatos, Catal. Today 110 (2005) 114.
[25] S. Fiorot, C. Galetti, S. Specchia, G. Saracco, V. Specchia, Int. J. Chem. Reactor Eng. 5 (2007) A113.
[26] S.H. Lee, J. Han, K.-Y. Lee, J. Power Sources 109 (2002) 394.
[27] S. Srinivas, E. Gulari, Catal. Commun. 7 (2006) 819.
[28] R.K. Ahluwalia, Q. Zhang, D.J. Chmielewski, K.C. Lauzze, M.A. Inbody, Catal. Today 99 (2005) 271.
[29] S. Roychoudhury, M. Lyubovski, A. Shabbir, J. Power Sources 152 (2005) 75.
[30] S. Zhou, Z. Yuan, S. Wang, Int. J. Hydrogen Energy 31 (2006) 924.
[31] P. Chin, X. Sun, G.W. Roberts, J.J. Spivey, Appl. Catal. A 302 (2006) 22.
[32] C.D. Dudfield, R. Chen, P.L. Adock, Int. J. Hydrogen Energy 26 (2001) 763.
[33] E. Lopez, G. Kolios, G. Eigenberger, Chem. Eng. Sci. 62 (2007) 5598.
[34] G. Kolb, J. Schürer, D. Tiemann, M. Wichert, R. Zapf, V. Hessel, H. Löwe, J. Power Sources 171 (2007) 198.
[35] W.E. TeGrotenhuis, D.L. King, K.P. Brooks, B.J. Holladay, R.S Wegeng, 6th International Conference on Microreaction Technology IMRET 6, New Orleans, USA, 11–14 March, 2002.
[36] T. Baier, G. Kolb, Chem. Eng. Sci. 62 (2007) 4602.
[37] G. Kolb, D. Tiemann, Mikroverdampfer, DE 10 2005 017 452 B4 2008.01.31, Germany, 2006.
[38] G. Kolb, T. Baier, J. Schürer, D. Tiemann, A. Ziogas, H. Ehwald, P. Alphonse, Chem. Eng. J. 137 (2008) 653.
[39] Z. Pors, J. Pasel, A. Tschauder, R. Dahl, R. Peters, D. Stolten, Fuel Cells 2 (2008) 129.
[40] S. Yoon, I. Kang, J. Bae, Int. J. Hydrogen Energy 33 (2008) 4780.
[41] M. Nilsson, L.J. Petterson, Ind. Eng. Chem. Res., submitted for publication.
[42] L. Hartmann, K. Lucka, H. Köhne, J. Power Sources 118 (2003) 286.
[43] Y. Choi, H.G. Stenger, J. Power Sources 129 (2004) 246.
[44] M. O'Connell, G. Kolb, K.P. Schelhaas, J. Schürer, D. Tiemann, A. Ziogas, V. Hessel, Int. J. Hydrogen Energy 34 (2009) 6290.
[45] M.O'Connell, D. Tiemann, A. Ziogas, G. Kolb, Int. J. Hydrogen Energy, in preparation.